Neurovascular Unit Model

Documentation for Code "OO-NVU Version 2.0"

A merged NVC model of a neuron, astrocyte, smooth muscle cell, endothelial cell and the mechanical vessel response.

by Emiel van Disseldorp Katharina Dormanns Sanne van der Lelij
Joerik de Ruijter Michelle Louise Goodman Eva Waldhauser
Moritz Burger Kon Zakkaroff Tim David*

May 25, 2015

*Corresponding author, Tim.david@canterbury.ac.nz

Contents

1 Release notes

1.1 Changes to the previous version

This is where changes should be listed.

1.2 Corrections

A mistake was discovered in NVU1.0 for the equation used to describe the K^+ concentration in the synaptic cleft. The original equation subtracted the change in astrocytic K^+ concentration from the K^+ influx from the neuron. This was incorrect since not all channels lead from the astrocyte to the synaptic cleft. The BK-channel describes the flux from the astrocyte to the perivascular space, and therefore this flux was added to the equation. Fortunately, this mistake led to very small changes, and it did not significantly change the model outcomes. Figure 1 shows the old and the corrected results for the flux through the BK-channel, and it is clear that they practically overlap.

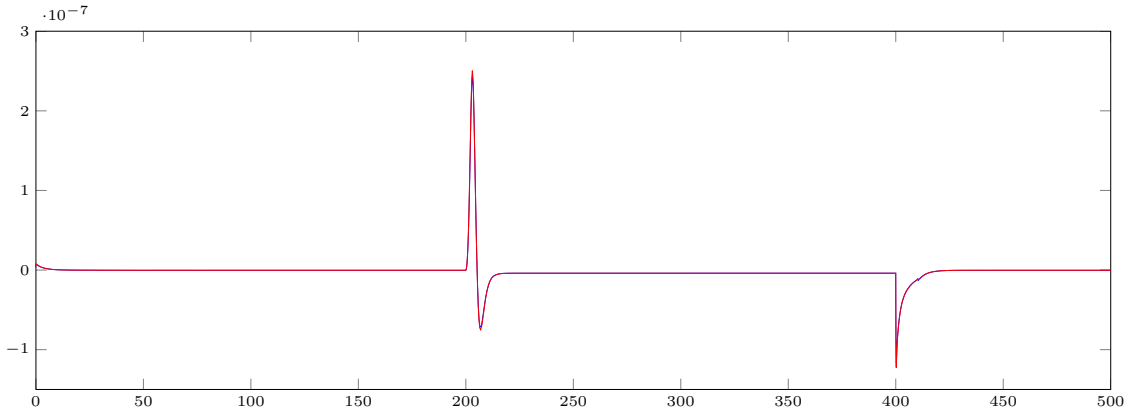

Figure 1: The flux through the BK-channel in µM m/s for the old (blue) and corrected (red) simulation

2 Code Structure

The three core classes, the `Astrocyte`, `SMCEC` and `WallMechanics`, correspond to the components of the NVU model, namely the astrocyte model, the SMC and EC model, and the mechanical contraction cell model. For a given model component, all fluxes and ODEs are grouped together in the code of the corresponding class. The `NVU` class uses the three core component classes to collect the state variable and derivatives values and pass them to the `ode15s` solver for stiff problems. All classes in OO-NVU code are subclasses of the MATLAB's `handle` class which makes them appear as reference object to avoid unnecessary object duplication on assignment. Figure 2 shows the public interfaces for all OO-NVU classes.

For a proper OO development and complexity management in the future the Astrocyte, SMCEC and the WallMechanics classes should have a common superclass with the shared interface (at least) and functionality. –Kon

The following features apply to the `Astrocyte`, `SMCEC` and `WallMechanics` classes:

1. The core classes rely on the class constructors to initialise the parameters with the help of the class-specific function parse_inputs(varangin). The constructors also initialise the variable indices, initial conditions and the output indices.

2. In every core class the `rhs` method contains the algebraic and state variables, as well as the corresponding equations.

3. The `shared(self, ~, u)` method, where present, provides the access to the shared algebraic or state variables used as input variables in the other model components where appropriate.

The code in the file `nvu_script.m` provides a number of use-cases for running the NVU model. The code Listing 1 shows an example of setting the options for the ODE solver `ode15s` specifying the `odeopts` parameter, however the code works well with default tolerances. The `simulate()` method of the `NVU` class start the simulation.

Listing 1: Initialisation of the NVU model components.

```
odeopts = odeset('RelTol', 1e-03, 'AbsTol', 1e-03, 'MaxStep', 1, ...
    'Vectorized', 1);

nv = NVU(Astrocyte(), ...
WallMechanics(), ...
SMCEC('J_PLC', 0.18), ...
'odeopts', odeopts);

nv.simulate()
```

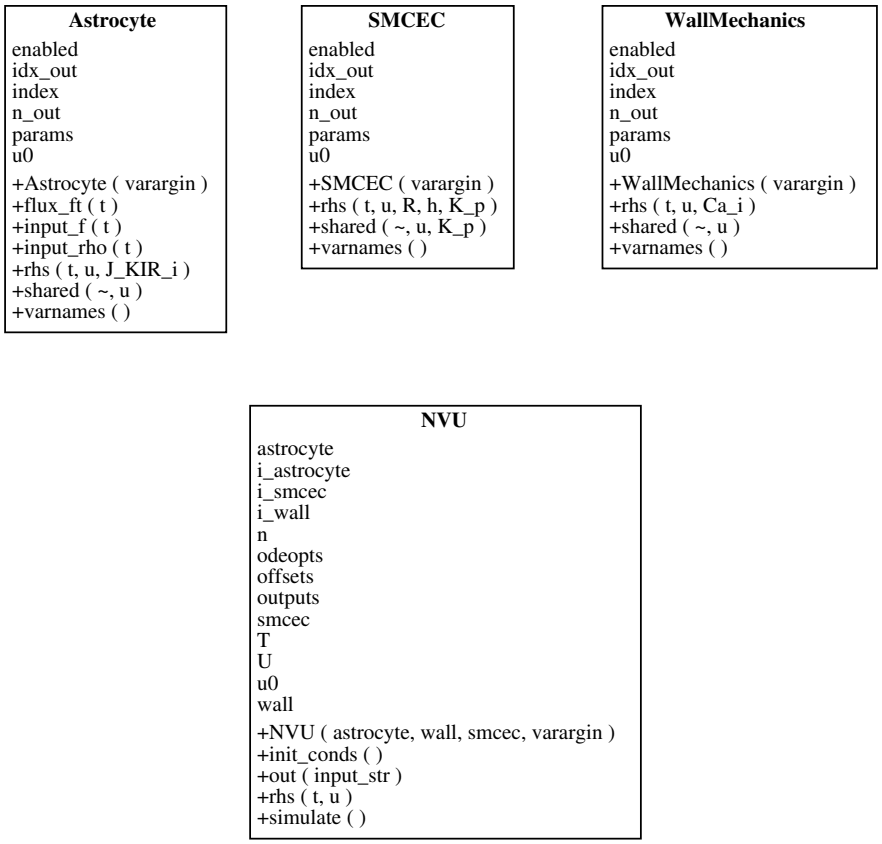

Figure 2: UML class diagram for the OO NVU code.

This is the first draft of this section. Suggestions as to what needs to be expanded further? Include more code listings? –Kon

Remove the code structure files used in the previous documentation version when this version is done. –Kon

3 Introduction

3.1 Neurovascular Unit

The cerebral cortex, a highly complex component of the human brain and part of the grey matter (*substantia grisea*), mainly consists of neurons (NEs), unmyelinated axons and glial cells such as astrocytes (ACs). It forms the outer layer of *cerebrum* and *cerebellum* and is veined with capillary blood vessels that provide the brain tissue with glucose and oxygen (Shipp [9]). These arterioles are surrounded by endothelial cells (ECs) that form a thin layer on the interior surface of arterioles (*intima*). The outer layer of the arteriole consists of smooth muscle cells (SMCs), which are aligned in circumferential direction. They define the contractile unit of the vessel and regulate its diameter by contraction and dilation.

A neurovascular unit (NVU) defined in this research includes one cell of each of the described types and is graphically pictured in Figure 4.

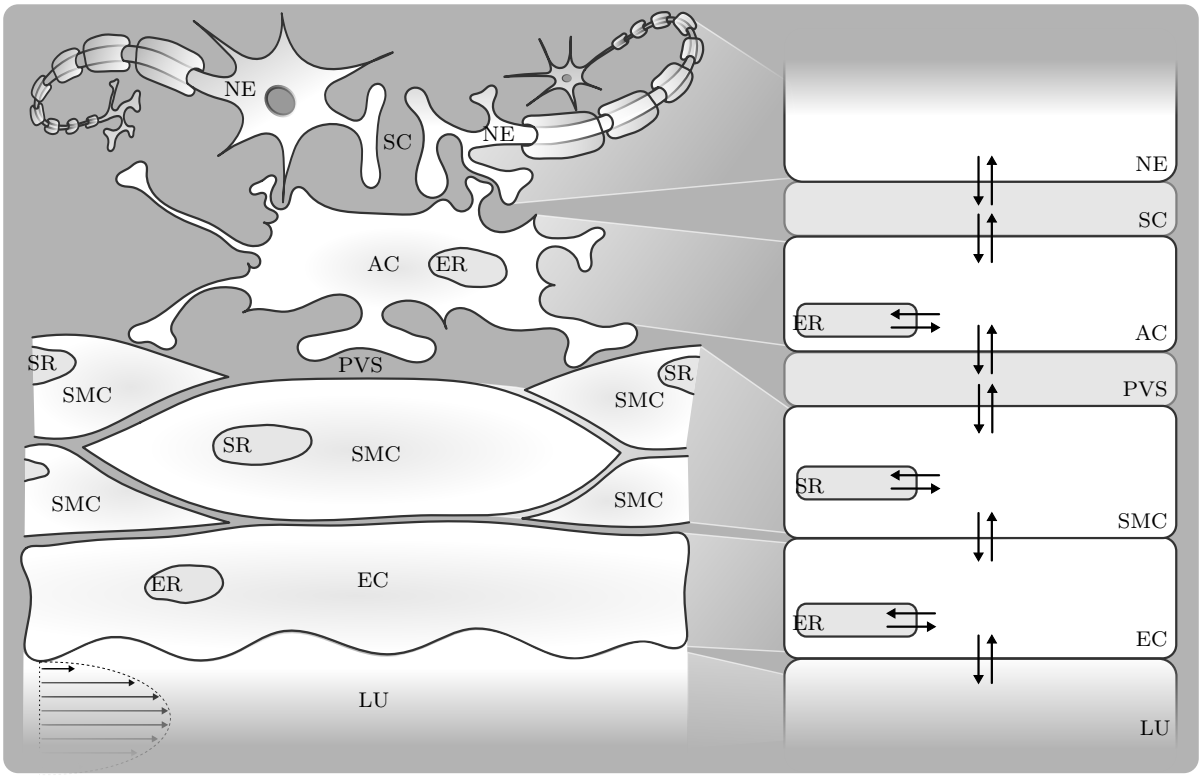

Figure 3: **Overview of different cells and domains that form a neurovascular unit.** NE - Neuron, SC - Synaptic Cleft, AC - Astrocyte, ER - Endoplasmic Reticulum, PVS - Perivascular Space, SMC - Smooth Muscle Cell, SR - Sarcoplasmic Reticulum, EC - Endothelial Cell, LU - Lumen with indicated blood flow. Intercellular communication via the exchange of ions is indicated by arrows.

Each of the cell types and the spaces in between play an important role within the process of neurovascular coupling (NVC, see Section 3.2). The synaptic cleft (SC) is the space between an axon terminal and dendrite of two different NEs in which neurotransmitters are released. It is enclosed by the star-shaped AC that can take up released neurotransmitters. Protoplasmic ACs are polarized cells which can temporarily buffer extracellular K^+, which is one of the key mechanisms within NVC. The astrocytic endoplasmatic reticulum (ER), an isolated space in the cytosol, contains IP_3-sensitive Ca^{2+} channels, which can release Ca^{2+}-ions into the cytosol. The perivascular space (PVS) is located between the end feet of an AC and the arteriole. In the PVS, ion exchange occurs between the arterial wall and the AC. The ECs form a monolayer on the luminal side of the vessel in which all cells are aligned in the direction of the flow. It prevents passive diffusion of bigger molecules, while small ones, such as O_2, Ca^{2+} or IP_3, can pass through. It also functions as an active organ sensing wall shear stress which plays an important role in the NO-mediated pathway. Together with the SMC layer the endothelium forms the blood brain barrier (BBB), the physical frontier between brain tissue and blood vessel. SMC contraction occurs by actin and myosin filaments forming cross-bridges. The rate of contraction is dependent on the SMC cytosolic Ca^{2+} concentration.

3.2 Neurovascular Coupling

Neurovascular coupling (NVC), or functional hyperaemia, describes the local vasodilation and -contraction due to neuronal activation. The change in the vessel diameter (vasoreactivity) controls the blood flow and thereby the cerebral supply of oxygen and glucose.

Each cell type plays an important specific role during the process of NVC. Communication between cells is based on an exchange of ions through pumps and channels. These ion fluxes contribute to changes in cytosolic and intercellular species concentration and cell membrane potentials.

There are several pathways that can lead to vasocontraction or -dilation and are mediated by different signalling molecules, such as K^+, Ca^{2+}, EET, NO and 20-HETE. Neurotransmitters are released by the NE into the SC and can bind to receptors on dendrites of other neurons and astrocytes. This leads to a cascade of chemical reactions and the opening and closing of ion channels which influences the fluxes and concentrations.

3.3 Mathematical Approach

The physiological models are based on a set of differential equations that describe the mass conservation of ions and molecules passing from one cell or domain to another. The simulations describe time-dependent ion fluxes and changes in membrane potential modelled by reaction rates that describe the kinetics which are physiologically validated by experimental data from the literature. This approach assumes homogeneous behaviour of a variable in a certain subdomain i.e. the spatial gradient of a variable in every subdomain is negligible.

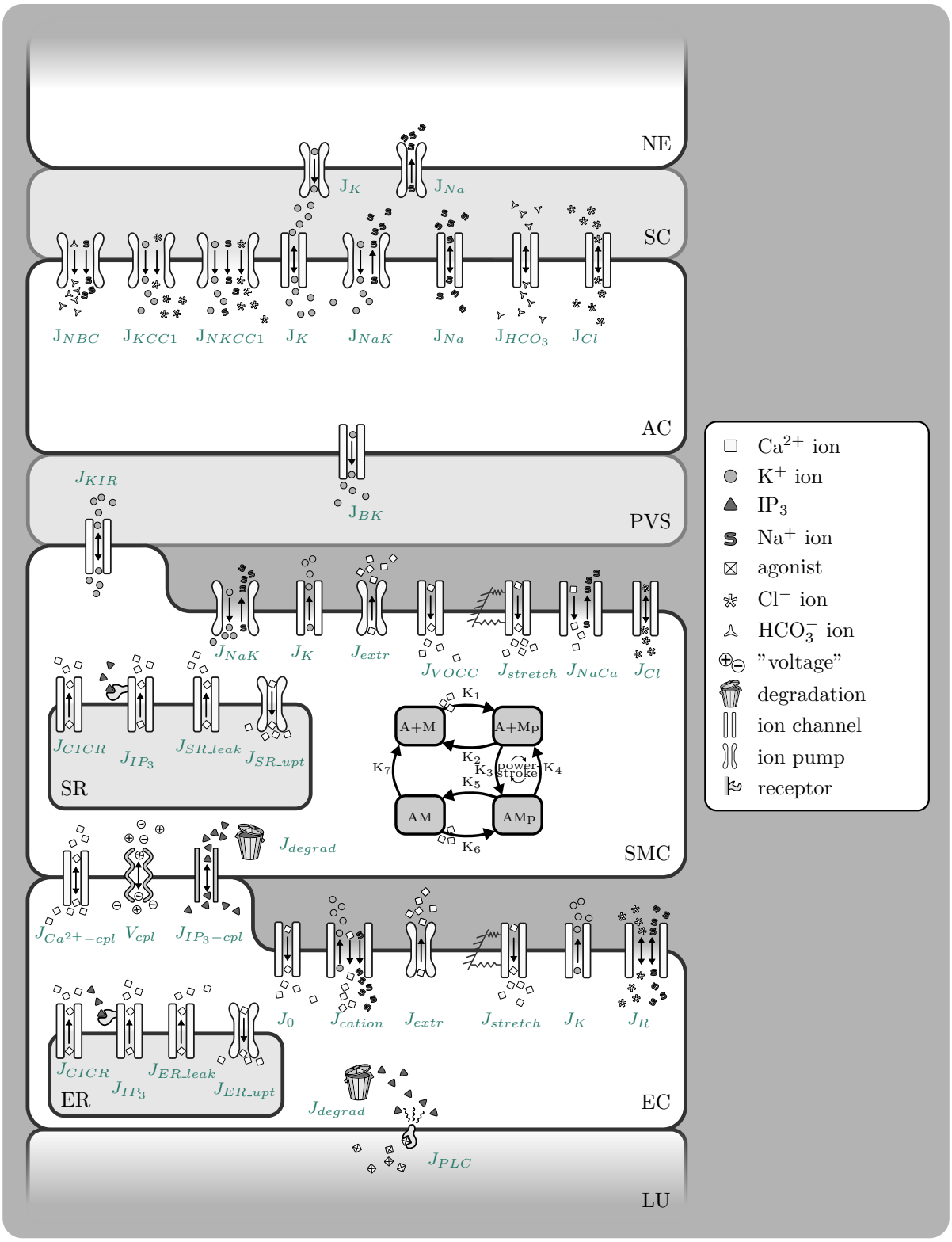

Figure 4: **Overview of model.** NE - Neuron, SC - Synaptic Cleft, AC - Astrocyte, ER - Endoplasmic Reticulum, PVS - Perivascular Space, SMC - Smooth Muscle Cell, SR - Sarcoplasmic Reticulum, EC - Endothelial Cell, LU - Lumen.

4 Results

4.1 OO-NVU 2.0

Potassium input signal (figure 5)

At the top the neuronal K^+ input signal is shown. This input signal is pumped into the SC by the NE. As a result of that, there is more K^+ taken up by the AC in the beginning of the input pulse, and released at the end of the input pulse. In the second graph the membrane potential of the AC is shown over time. When the K^+ concentration in the SC is increased the membrane voltage depolarises and when the K^+ concentration in the SC decreases the membrane potential repolarises again. In the third graph the fluxes into the PVS are shown. In blue the flux by the astrocytic BK channel, and in green the flux by the KIR channel in the SMC is shown. The drop in the middle of the KIR flux is caused because the SMC becomes in a oscillatory state and therefore the efflux by the KIR channel follows the Ca^{2+} waves inside the SMC. The bottom figure shows the K^+ concentration in the PVS.

Neurovascular Coupling Overview (figure 6)

This figure describes the main pathway from the synaptic cleft to the radius change. It starts with a K^+ concentration in the synaptic cleft, followed by the flux trough the BK-channel determined in the astrocyte, leading to an increased K^+ concentration in the perivascular space. This causes an increased K^+ influx trough the KIR channel, changing the membrane voltage of the SMC. The Ca^{2+} flux through the VOCC increases, decreasing the Ca^{2+} concentration in the SMC and thereby inducing vasodilation.

AC State Variables (figure 7)

The graphs display the concentrations of K^+, Ca^{2+}, Cl and HCO3 in the astrocyte and K^+ in the SC and PVS. These concentrations, together with the membrane voltage contribute to the opening of the BK-channel in their own way. The open state of the BK channel determines the potassium flux from the astrocyte to the perivascular spcace, where it induces vascular contraction.

AC Fluxes (figure 8)

All ion fluxes that enter or leave the astrocyte.

SMC EC State Variables and Coupling (figure 9)

The graphs in this figure shows the solutions of the differential equations of the SMC and EC, including the intracellular Ca^{2+} concentration, the IP_3 concentration, the sarcoplasmic (SMC) or endoplasmic (EC) Ca^{2+} concentration, the membrane voltage and the coupling fluxes between EC and SMC.

SMC Fluxes (figure 10)

In these figures the coupling and the fluxes in the SMC are shown. When one of the fluxes is negative, it means that the direction of the flux is in the opposite than it is defined in the equations. These figures show that when the neuronal signal is given, the VOCC closes and that the SMC contracts.

EC Fluxes (figure 11)

All ion fluxes that enter or leave the EC.

Contraction Model and Radius (figure 12)

In this figure the fraction of the four states (M, Mp, AMp, AM) of myosin in the SMC are shown at the top. At the bottom left the fraction of attached cross bridged myosin (the sum of AM and AMp) is shown. And at the bottom right the radius is plotted over time. The increase in vessel diameter is in the expected order of magnitude.

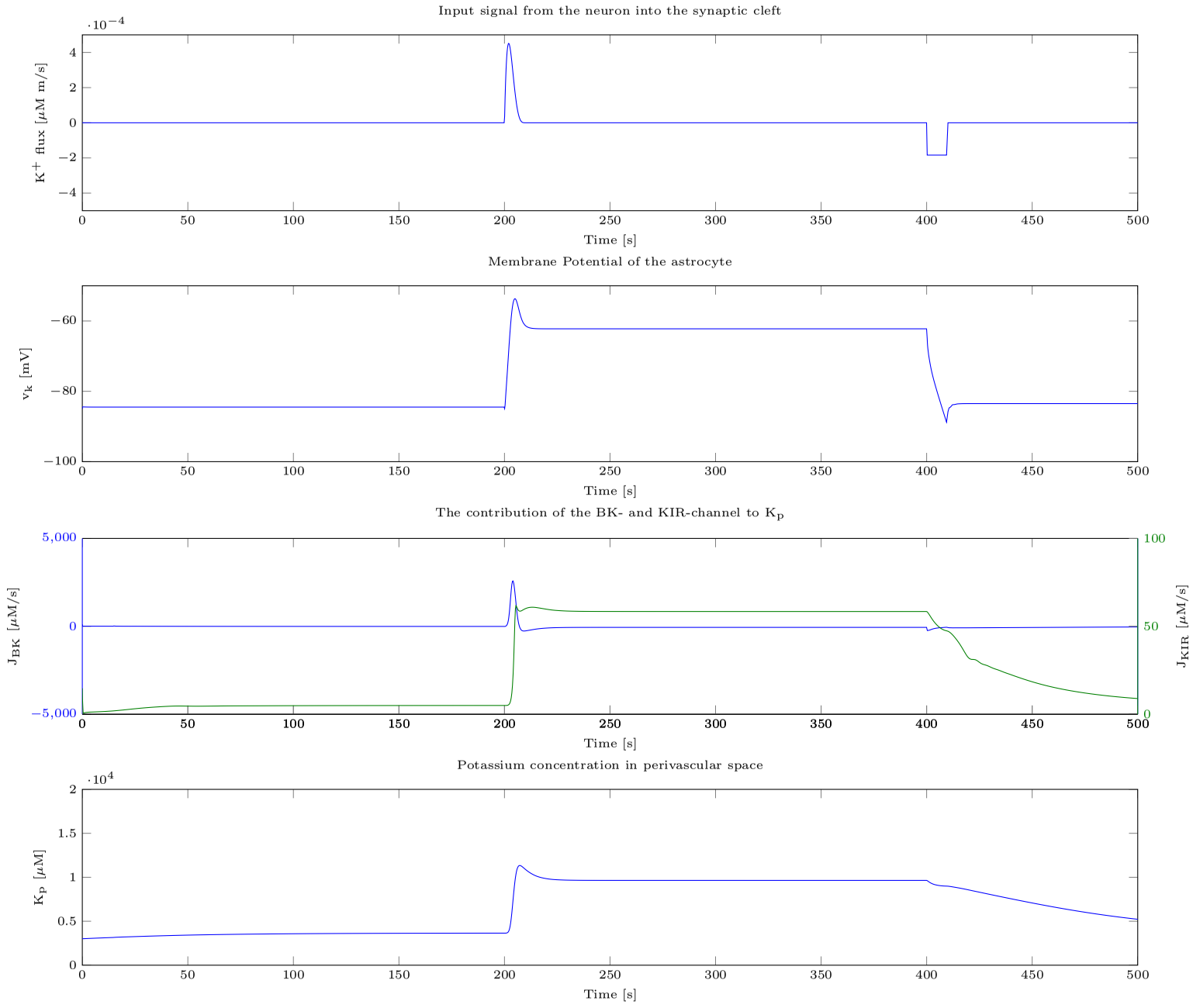

Figure 5: The input signal.

Neurovascular Coupling Overview.png

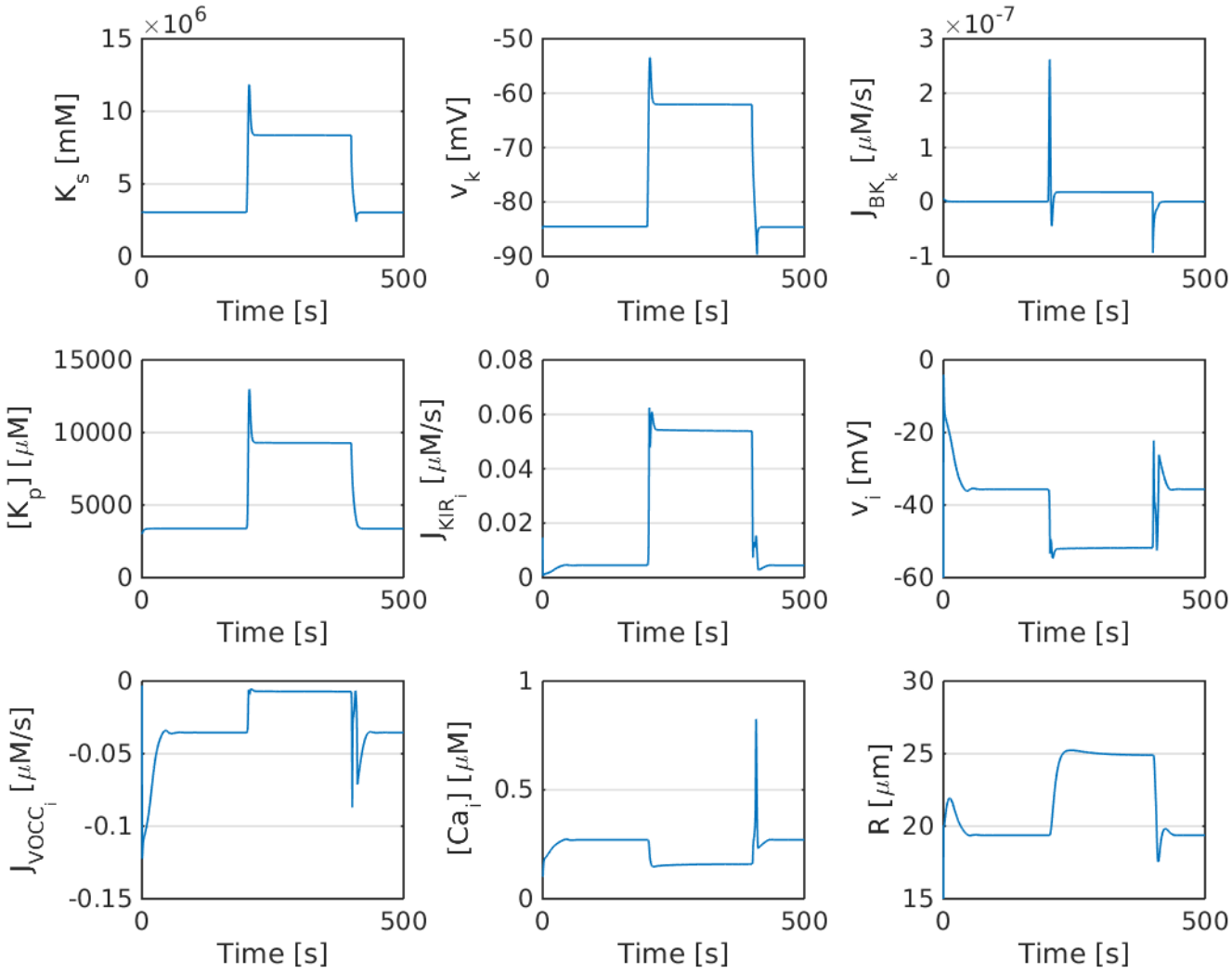

Figure 6: Neurovascular Coupling Overview.

AC State Variables.png

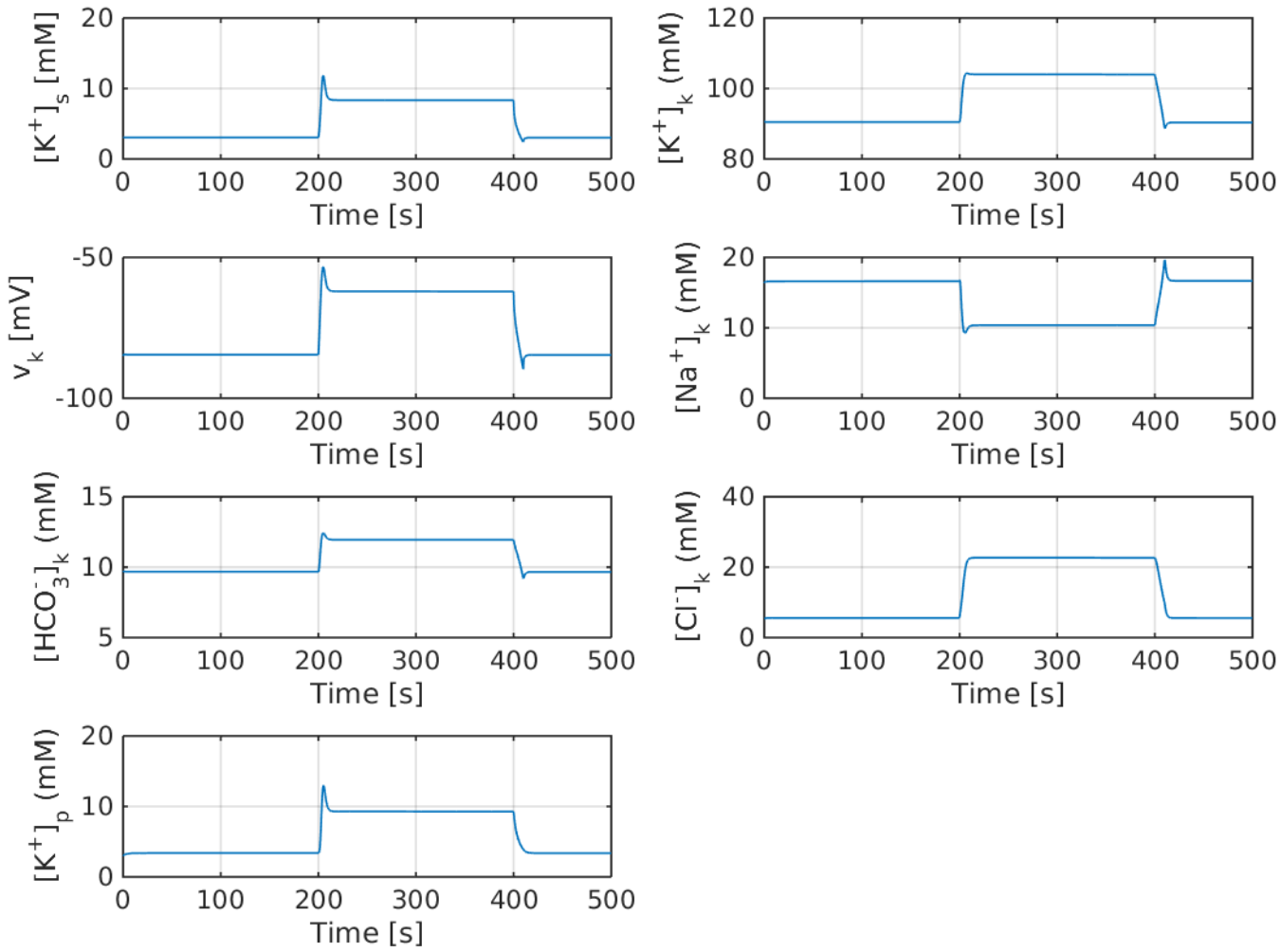

Figure 7: AC State Variables.

AC Fluxes.png

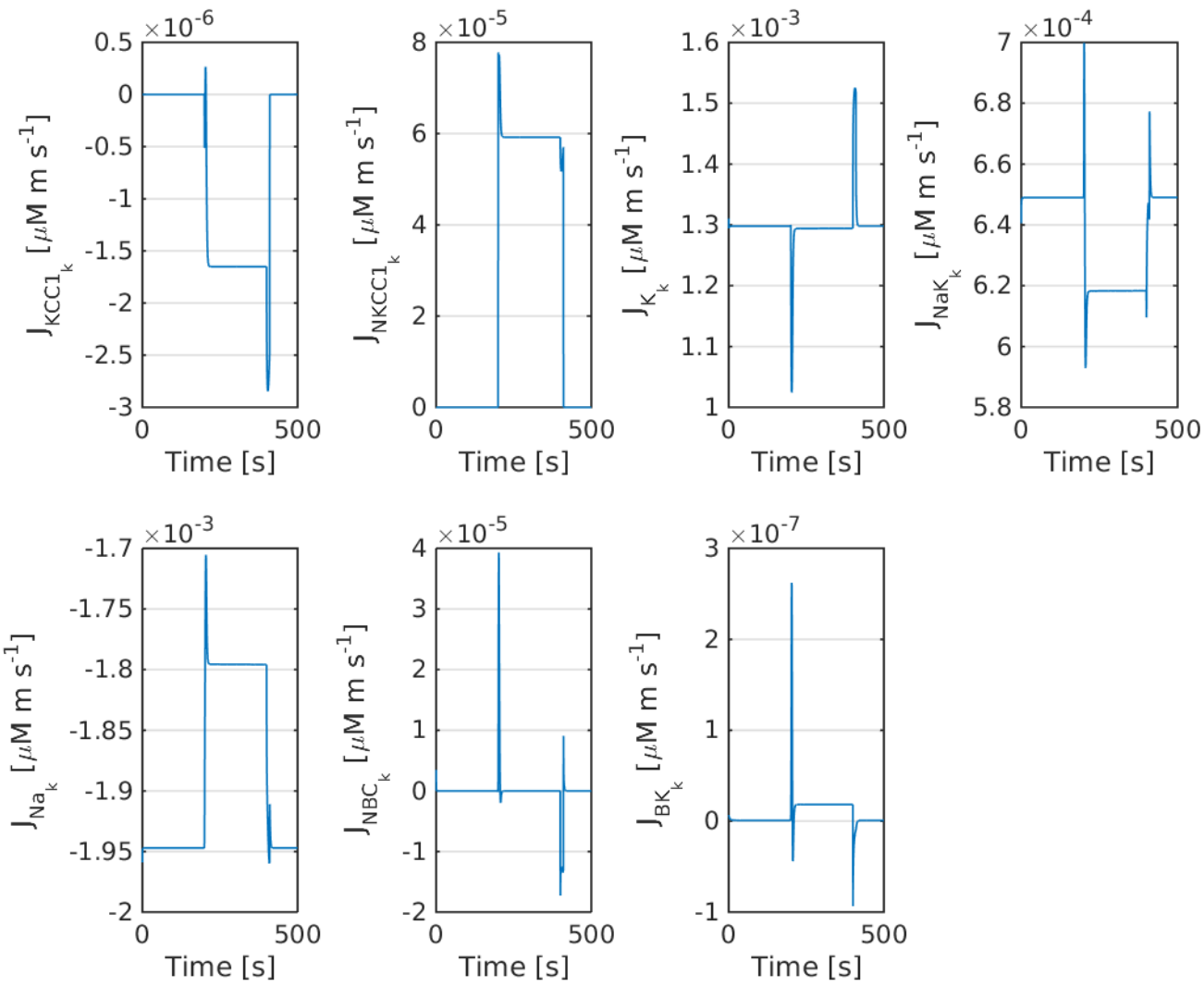

Figure 8: AC Fluxes.

SMC EC State Variables and Coupling.png

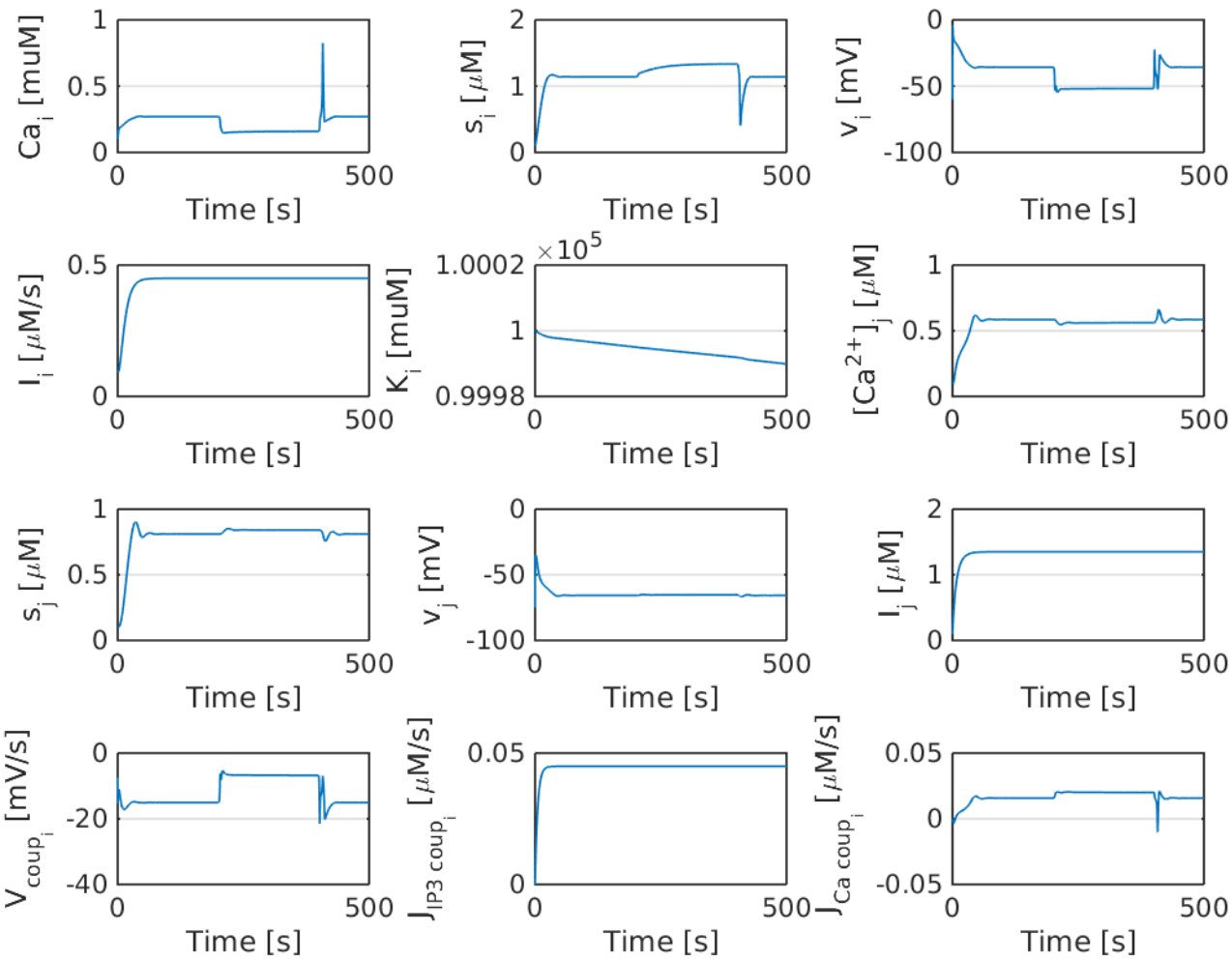

Figure 9: SMC EC State Variables and Coupling.

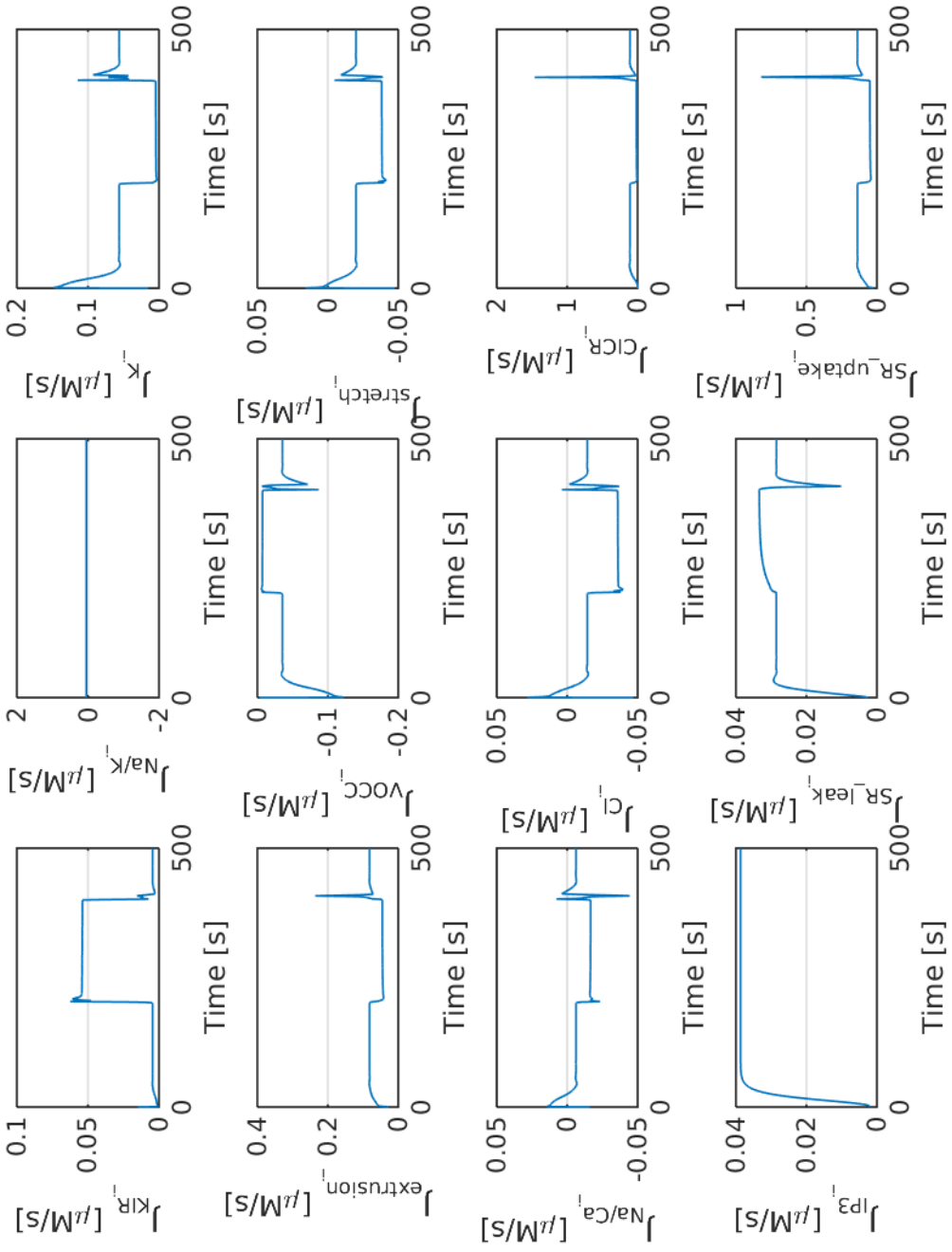

Figure 10: SMC Fluxes.

EC Fluxes.png

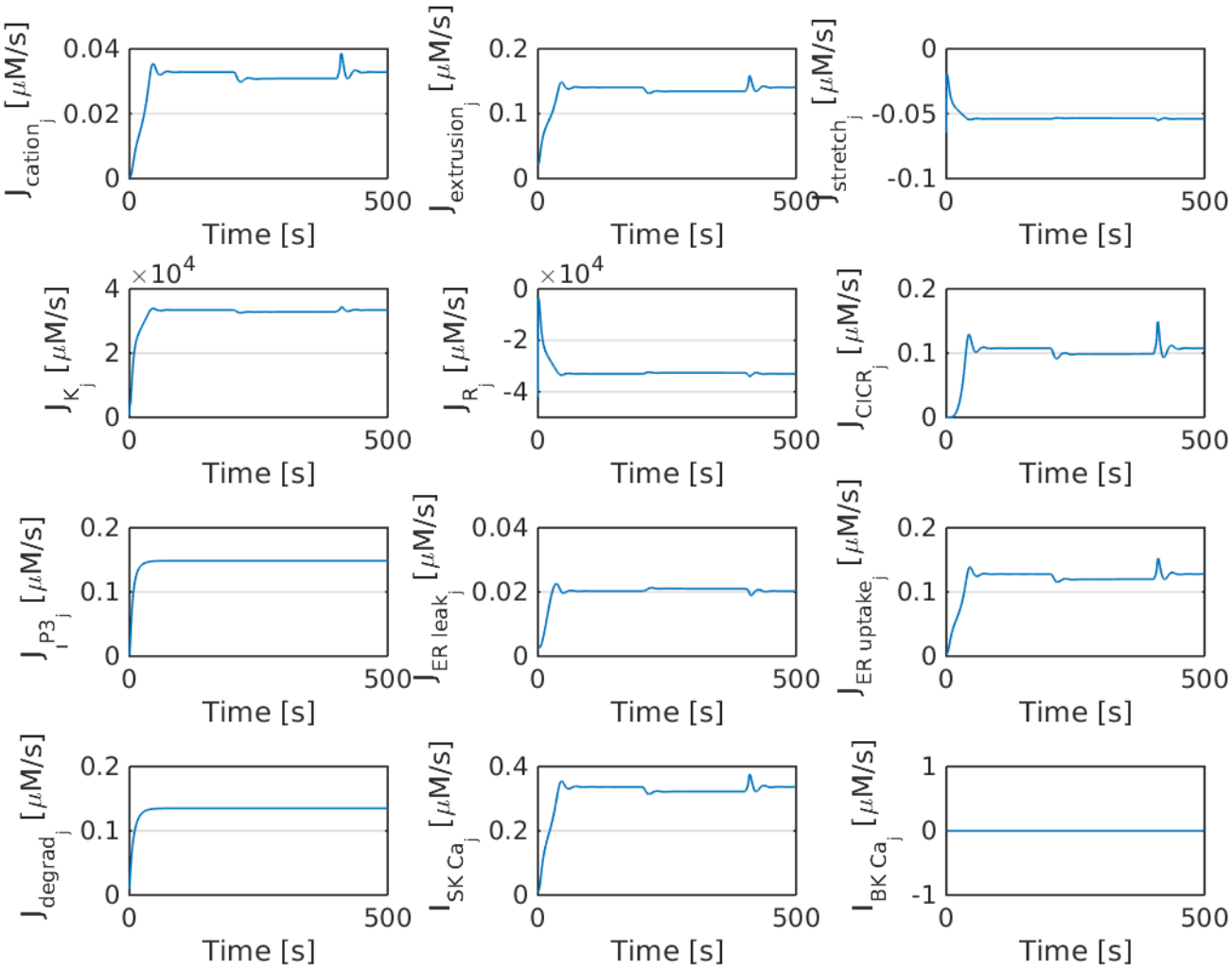

Figure 11: EC Fluxes.

Contraction Model and Radius.png

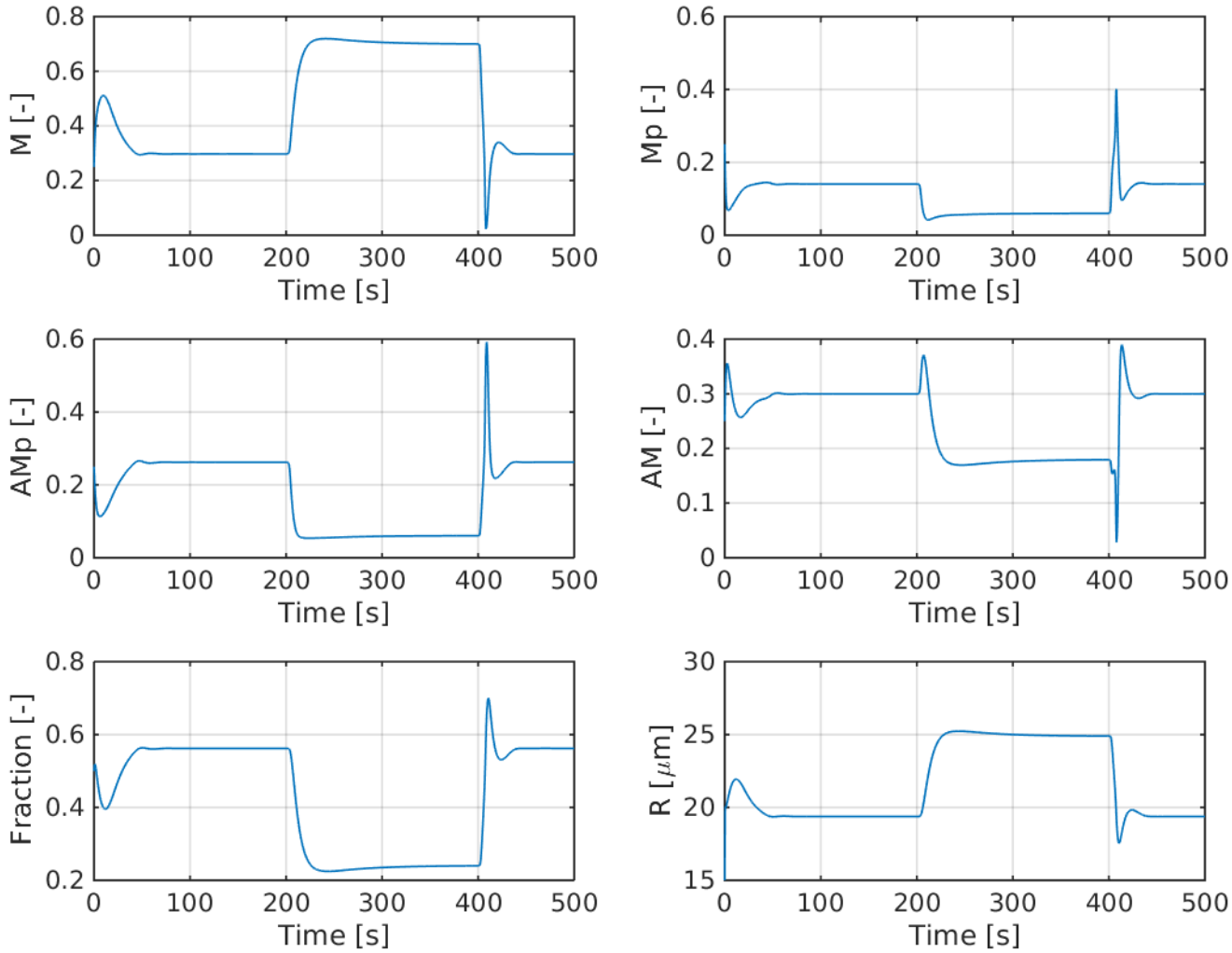

Figure 12: Contraction Model and Radius.

5 Equations

Some units need to be corrected in this documentation!

5.1 The Neuron and Astrocyte Model

Input signals

Neuronal K^+ input signal (-):
For $t < t_0$ and $t > t_3$:

$$f(t) = 0 \tag{1}$$

For $t_0 \leq t \leq t_1$:

$$f(t) = F_{input} \frac{(\alpha + \beta - 1)!}{(\alpha - 1)!(\beta - 1)!} \left(\frac{1 - (t - t_0)}{\Delta t} \right)^{\beta - 1} \left(\frac{t - t_0}{\Delta t} \right)^{\alpha - 1} \tag{2}$$

For $t_1 \leq t \leq t_2$:

$$f(t) = 0 \tag{3}$$

For $t_2 \leq t \leq t_3$:

$$f(t) = -F_{input} \tag{4}$$

t_0	Start of neuronal pulse	200 s	
t_1	End of neuronal pulse	210 s	
t_2	Start of back-buffering	230 s	
t_3	End of back-buffering	240 s	
F_{input}	Amplitude scaling factor	2.5	
α	Gamma distribution constant	2	ME[1]
β	Gamma distribution constant	5	ME
Δt	Time-scaling factor	10 s	

Scaling

AC volume-area ratio (in m):

$$\frac{\mathrm{d}R_k}{\mathrm{d}t} = L_p(Na_k + K_k + Cl_k + HCO_{3_k} - Na_s - K_s - Cl_s - HCO_{3_s} + \frac{X_k}{R_k}) \tag{5}$$

SC volume-surface ratio (in m):

$$R_s = R_{tot} - R_k \tag{6}$$

[1] Model Estimation

L_p	Total water permeability per unit area of the astrocyte	2.1×10^{-9} mμM^{-1}s^{-1}	[8]
X_k	Number of negatively charged impermeable ions trapped within the astrocyte divided by the astrocyte membrane area	12.41×10^{-3} μM m	[8]
R_{tot}	Total volume surface ratio AC+SC	8.79×10^{-8} m	[8]

Conservation Equations

Synaptic Cleft

K^+ concentration in the SC (times the SC volume-area ratio R_s; in μM m):

$$\frac{\mathrm{d}N_{K_s}}{\mathrm{d}t} = k_C f(t) - \frac{\mathrm{d}N_{K_k}}{\mathrm{d}t} - J_{BK_k} \tag{7}$$

Na^+ concentration in the SC (times the SC volume-area ratio R_s; in μM m):

$$\frac{\mathrm{d}N_{Na_s}}{\mathrm{d}t} = -k_C f(t) - \frac{\mathrm{d}N_{Na_k}}{\mathrm{d}t} \tag{8}$$

HCO_3 concentration in the SC (times the SC volume-area ratio R_s; in μM m):

$$\frac{\mathrm{d}N_{HCO_{3_s}}}{\mathrm{d}t} = -\frac{\mathrm{d}N_{HCO_{3_k}}}{\mathrm{d}t} \tag{9}$$

k_C	Input scaling parameter	7.35×10^{-5} μM m s^{-1}	[8]

Astrocyte

K^+ concentration in the AC (times the AC volume-area ratio R_k; in μM m):

$$\frac{\mathrm{d}N_{K_k}}{\mathrm{d}t} = -J_{K_k} + 2J_{NaK_k} + J_{NKCC1_k} + J_{KCC1_k} - J_{BK_k} \tag{10}$$

Na^+ concentration in the AC (times the AC volume-area ratio R_k; in μM m):

$$\frac{\mathrm{d}N_{Na_k}}{\mathrm{d}t} = -J_{Na_k} - 3J_{NaK_k} + J_{NKCC1_k} + J_{NBC_k} \tag{11}$$

HCO_3 concentration in the AC (times the AC volume-area ratio R_k; in μM m):

$$\frac{\mathrm{d}N_{HCO_{3_k}}}{\mathrm{d}t} = 2J_{NBC_k} \tag{12}$$

Cl concentration in the AC (times the AC volume-area ratio R_k; in μM m):

$$\frac{\mathrm{d}N_{Cl_k}}{\mathrm{d}t} = \frac{\mathrm{d}N_{Na_k}}{\mathrm{d}t} + \frac{\mathrm{d}N_{K_k}}{\mathrm{d}t} - \frac{\mathrm{d}N_{HCO_{3_k}}}{\mathrm{d}t} \tag{13}$$

Open probability of the BK channel (non-dim.):

$$\frac{\mathrm{d}w_k}{\mathrm{d}t} = \phi_w \left(w_\infty - w_k\right) \tag{14}$$

Perivascular Space

K^+ concentration in the PVS (in µM):

$$\frac{\mathrm{d}K_p}{\mathrm{d}t} = \frac{J_{BK_k}}{R_k R_{pa}} + \frac{J_{KIR_i}}{R_{ps}} \tag{15}$$

R_{pa}	Volume ratio of PVS to AC	10^{-3} [-]	[7]
R_{ps}	Volume ratio of PVS to SMC	10^{-3} [-]	[7]

Fluxes

K^+ flux (times the AC volume-area ratio R_k; in µM m s^{-1}):

$$J_{K_k} = \frac{g_{K_k}}{F}(v_k - E_{K_k}) \tag{16}$$

Na^+ flux (times the AC volume-area ratio R_k; in µM m s^{-1}):

$$J_{Na_k} = \frac{g_{Na_k}}{F}(v_k - E_{Na_k}) \tag{17}$$

Na^+ and HCO_3 flux through the NBC channel (times the AC volume-area ratio R_k; in µM m s^{-1}):

$$J_{NBC_k} = \frac{g_{NBC_k}}{F}\left(v_k - E_{NBC_k}\right) \tag{18}$$

Cl and K^+ flux through the KCC1 channel (times the AC volume-area ratio R_k; in µM m s^{-1}):

$$J_{KCC1_k} = C_{input}\frac{g_{KCC1_k}}{F}\frac{R_g T}{F} ln\left(\frac{K_s Cl_s}{K_k Cl_k}\right) \tag{19}$$

Na^+, K^+ and Cl flux through the NKCC1 channel (times the AC volume-area ratio R_k; in µM m s^{-1}):

$$J_{NKCC1_k} = C_{input}\frac{g_{NKCC1_k}}{F}\frac{R_g T}{F} ln\left(\frac{Na_s K_s {Cl_s}^2}{Na_k K_k {Cl_k}^2}\right) \tag{20}$$

Flux through the sodium potassium pump (times the AC volume-area ratio R_k; in µM m s^{-1}):

$$J_{NaK_k} = J_{NaK_{max}}\frac{{Na_k}^{1.5}}{{Na_k}^{1.5} + {K_{Na_k}}^{1.5}}\frac{K_s}{K_s + K_{K_s}} \tag{21}$$

K^+ flux through the BK channel (times the AC volume-area ratio R_k; in µM m s^{-1}):

$$J_{BK_k} = \frac{g_{BK_k}}{F} w_k \left(v_k - E_{BK_k}\right) \tag{22}$$

F	Faraday's constant	9.649×10^4 C mol^{-1}	
R_g	Gas constant	8.315 J mol^{-1}K^{-1}	
T	Temperature	300 K	
g_{K_k}	Specific ion conductance of potassium	40×10^3 Ω^{-1}m^{-2}	[8]
g_{Na_k}	Specific ion conductance of sodium	1.314×10^3 Ω^{-1}m^{-2}	[8]
g_{NBC_k}	Specific ion conductance of the NBC cotransporter	7.57×10^2 Ω^{-1}m^{-2}	[8]
g_{KCC1_k}	Specific ion conductance of the KCC1 cotransporter	10 Ω^{-1}m^{-2}	[8]
g_{NKCC1_k}	Specific ion conductance of the NKCC1 cotransporter	55.4 Ω^{-1}m^{-2}	[8]
$J_{NaK_{max}}$	Maximum flux through the NaKATPase pump	1.42×10^{-3} µMms^{-1}	[8]
g_{BK_k}	Specific ion conductance of the BK channel	1.16×10^3 Ω^{-1}m^{-2}	[2]
C_{input}	Block function to switch the channel on and off	0 ; 1 [-]	
K_{Na_k}	Michaelis-Menten constant	10^4 µM	
K_{K_s}	Michaelis-Menten constant	1.5×10^3 µM	

Additional Equations

Synaptic Cleft

Cl concentration (times the SC volume-area ratio R_s; in µM m):

$$N_{Cl_s} = N_{Na_s} + N_{K_s} - N_{HCO_{3s}} \tag{23}$$

Astrocyte

Membrane voltage of the AC (V):

$$v_k = \frac{g_{Na_k}E_{Na_k} + g_{K_k}E_{K_k} + g_{Cl_k}E_{Cl_k} + g_{NBC_k}E_{NBC_k} + g_{BK_k}w_kE_{BK_k} - J_{NaK_k}F\times10^3}{g_{Na_k} + g_{K_k} + g_{Cl_k} + g_{NBC_k} + g_{BK_k}w_k} \tag{24}$$

Nernst potential for the potassium channel (in mV):

$$E_{K_k} = \frac{R_gT}{z_KF}ln\left(\frac{K_s}{K_k}\right) \tag{25}$$

Nernst potential for the sodium channel (in mV):

$$E_{Na_k} = \frac{R_gT}{z_{Na}F}ln\left(\frac{Na_s}{Na_k}\right) \tag{26}$$

Nernst potential for the chloride channel (in mV):

$$E_{Cl_k} = \frac{R_gT}{z_{Cl}F}ln\left(\frac{Cl_s}{Cl_k}\right) \tag{27}$$

Nernst potential for the NBC channel (in mV):

$$E_{NBC_k} = \frac{R_gT}{z_{NBC}F}ln\left(\frac{Na_s{HCO_{3_s}}^2}{Na_k{HCO_{3_k}}^2}\right) \tag{28}$$

Nernst potential for the BK channel (in mV):

$$E_{BK_k} = \frac{R_g T}{z_K F} ln\left(\frac{K_p}{K_k}\right) \tag{29}$$

Equilibrium state BK-channel (-):

$$w_\infty = 0.5\left(1 + \tanh\left(\frac{v_k + v_6}{v_4}\right)\right) \tag{30}$$

Time constant associated with the opening of BK channels (in s^{-1}):

$$\phi_w = \psi_w \cosh\left(\frac{v_k + v_6}{2v_4}\right) \tag{31}$$

g_{Cl_k}	Specific ion conductance of chloride	0.879 $\Omega^{-1}\mathrm{m}^{-2}$	[8]
z_K	Valence of a potassium ion	1	
z_{Na}	Valence of a sodium ion	1	
z_{Cl}	Valence of a chloride ion	-1	
z_{NBC}	Effective valence of the NBC cotransporter complex	-1	
v_6	Voltage associated with the opening of half the population	22 mV	[2]
v_4	A measure of the spread of the distribution of the open probability of the BK channel	14.5 mV	[2]
ψ_w	A characteristic time for the open probability of the BK channel	2.664 s^{-1}	[2]

5.2 The Smooth Muscle Cell and Endothelial Cell Model

Conservation Equations

Smooth muscle cell

Cytosolic [Ca^{2+}] in the SMC (in µM):

$$\begin{aligned}\frac{\mathrm{d}[Ca^{2+}]_i}{\mathrm{d}t} = J_{IP_{3i}} - J_{SR_{uptake_i}} + J_{CICR_i} - J_{extrusion_i} + J_{SR_{leak_i}} \dots \\ - J_{VOCC_i} + J_{Na/Ca_i} + 0.1 J_{stretch_i} + J^{SMC-EC}_{Ca^{2+}-coupling_i}\end{aligned} \tag{32}$$

[Ca^{2+}] in the SR of the SMC (in µM):

$$\frac{\mathrm{d}[\widehat{Ca}^{2+}]_i}{\mathrm{d}t} = J_{SR_{uptake_i}} - J_{CICR_i} - J_{SR_{leak_i}} \tag{33}$$

Membrane potential of the SMC (in mV):

$$\begin{aligned}\frac{\mathrm{d}v_i}{\mathrm{d}t} = \gamma_i(-J_{Na/K_i} - J_{Cl_i} - 2J_{VOCC_i} - J_{Na/Ca_i} - J_{K_i} \dots \\ - J_{stretch_i} - J_{KIR_i}) + V^{SMC-EC}_{coupling_i}\end{aligned} \tag{34}$$

Open state probability of calcium-activated potassium channels (dim.less):

$$\frac{\mathrm{d}w_i}{\mathrm{d}t} = \lambda_i \left(K_{act_i} - w_i\right) \tag{35}$$

IP_3 concentration om the SMC (in µM):

$$\frac{\mathrm{d}[IP_3]_i}{\mathrm{d}t} = J^{SMC-EC}_{IP_3-coupling_i} - J_{degrad_i} \tag{36}$$

K^+ concentration in the SMC (in µM):

$$\frac{\mathrm{d}[K^+_i]}{\mathrm{d}t} = J_{Na/K_i} - J_{KIR_i} - J_{K_i} \tag{37}$$

γ_i	Change in membrane potential by a scaling factor	1970 $\mathrm{mV\mu M^{-1}}$	[5]
λ_i	Rate constant for opening	45.0 s^{-1}	[5]

Endothelial cell

Cytosolic Ca^{2+} concentration in the EC (in µM):

$$\begin{aligned}\frac{\mathrm{d}[Ca^{2+}]_j}{\mathrm{d}t} = J_{IP_{3j}} - J_{ER_{uptake_j}} + J_{CICR_j} - J_{extrusion_j} \cdots \\ + J_{ER_{leak_j}} + J_{cation_j} + J_{0_j} + J_{stretch_j} - J^{SMC-EC}_{Ca^{2+}-coupling_j}\end{aligned} \tag{38}$$

Ca^{2+} concentration in the ER in the EC (in µM):

$$\frac{\mathrm{d}[\widehat{Ca}^{2+}]_j}{\mathrm{d}t} = J_{ER_{uptake_j}} - J_{CICR_j} - J_{ER_{leak_j}} \tag{39}$$

Membrane potential of the EC (in mV):

$$\frac{\mathrm{d}v_j}{\mathrm{d}t} = -\frac{1}{C_{m_j}}(J_{K_j} + J_{R_j}) + V^{SMC-EC}_{coupling_j} \tag{40}$$

IP_3 concentration of the EC (in µM):

$$\frac{\mathrm{d}[IP_3]_j}{\mathrm{d}t} = J_{EC,IP_3} - J_{degrad_j} - J^{SMC-EC}_{IP_3-coupling_j} \tag{41}$$

C_{m_j}	Membrane capacitance	25.8 pF	[5]
J_{EC,IP_3}	IP_3 production rate	0.18 or 0.4 µM s^{-1}	[5]
J_{0_j}	leak		

F_i	Maximal rate of activation-dependent calcium influx	0.23 µM s^{-1}	[5]
K_{ri}	Half-saturation constant for agonist-dependent calcium entry	1 µM	[5]

Fluxes

Smooth muscle cell

Release of calcium from IP_3 sensitive stores in the SMC (in µM s^{-1}):

$$J_{IP_{3i}} = F_i \frac{[IP_3]_i^2}{K_{ri}^2 + [IP_3]_i^2} \tag{42}$$

Uptake of calcium into the sarcoplasmic reticulum (in µM s^{-1}):

$$J_{SR_{uptake_i}} = B_i \frac{[Ca^{2+}]_i^2}{c_{bi}^2 + [Ca^{2+}]_i^2} \tag{43}$$

B_i	SR uptake rate constant	2.025 µM s^{-1}	[5]
c_{bi}	Half-point of the SR ATPase activation sigmoidal	1.0 µM	[5]

Calcium-induced calcium release (CICR; in µM s^{-1}):

$$J_{CICR_i} = C_i \frac{[\widehat{Ca}^{2+}]_i^2}{s_{ci}^2 + [\widehat{Ca}^{2+}]_i^2} \frac{[Ca^{2+}]_i^4}{c_{ci}^4 + [Ca^{2+}]_i^4} \tag{44}$$

C_i	CICR rate constant	55 µM s^{-1}	[5]
s_{ci}	Half-point of the CICR Ca^{2+} efflux sigmoidal	2.0 µM	[5]
c_{ci}	Half-point of the CICR activation sigmoidal	0.9 µM	[5]

Calcium extrusion by Ca^{2+}-ATPase pumps (in µM s^{-1}):

$$J_{extrusion_i} = D_i[Ca^{2+}]_i \left(1 + \frac{v_i - v_d}{R_{di}}\right) \tag{45}$$

Leak current from the SR (in µM s^{-1}):

$$J_{SR_{leak_i}} = L_i[\widehat{Ca}^{2+}]_i \tag{46}$$

D_i	Rate constant for Ca^{2+} extrusion by the ATPase pump	0.24 s^{-1}	[5]
v_d	Intercept of voltage dependence of extrusion ATPase	-100.0 mV	[5]
R_{di}	Slope of voltage dependence of extrusion ATPase.	250.0 mV	[5]

L_i	Leak from SR rate constant	0.025 s^{-1}	[5]

Calcium influx through VOCCs (in µM s^{-1}):

$$J_{VOCC_i} = G_{Cai} \frac{v_i - v_{Ca_{1i}}}{1 + exp(-\left[\left(v_i - v_{Ca_{2i}}\right)/R_{Cai}\right])} \tag{47}$$

G_{Cai}	Whole-cell conductance for VOCCs	1.29×10^{-3} µM $mV^{-1}s^{-1}$	[5]
$v_{Ca_{1i}}$	Reversal potential for VOCCs	100.0 mV	[5]
$v_{Ca_{2i}}$	Half-point of the VOCC activation sigmoidal	-24.0 mV	[5]
R_{Cai}	Maximum slope of the VOCC activation sigmoidal	8.5 mV	[5]

Flux of calcium exchanging with sodium in the Na^+Ca^{2+} exchange (in µM s^{-1}):

$$J_{Na/Ca_i} = G_{Na/Ca_i} \frac{[Ca^{2+}]_i}{[Ca^{2+}]_i + c_{Na/Cai}} \left(v_i - v_{Na/Ca_i}\right) \tag{48}$$

$G_{Na/Cai}$	Whole-cell conductance for Na^+/Ca^{2+} exchange	3.16×10^{-3} µM $mV^{-1}s^{-1}$	[5]
$c_{Na/Cai}$	Half-point for activation of Na^+/Ca^{2+} exchange by Ca^{2+}	0.5 µM	[5]
$v_{Na/Cai}$	Reversal potential for the Na^+/Ca^{2+} exchanger	-30.0 mV	[5]

Calcium flux through the stretch-activated channels in the SMC (in µM s^{-1}):

$$J_{stretch_i} = \frac{G_{stretch}}{1 + exp\left(-\alpha_{stretch}\left(\frac{\Delta pR}{h} - \sigma_0\right)\right)} \left(v_i - E_{SAC}\right) \tag{49}$$

$G_{stretch}$	Whole cell conductance for SACs	6.1×10^{-3} µM $mV^{-1}s^{-1}$	[5]
$\alpha_{stretch}$	Slope of stress dependence of the SAC activation sigmoidal	7.4×10^{-3} $mmHg^{-1}$	[5]
Δp	Pressure difference	30 mmHg	ME
σ_0	Half-point of the SAC activation sigmoidal	500 mmHg	[5]
E_{SAC}	Reversal potential for SACs	-18 mV	[5]

Flux through the sodium potassium pump (in µM s^{-1}):

$$J_{Na/K_i} = F_{Na/K_i} \tag{50}$$

F_{Na/K_i}	Rate of the potassium influx by the sodium potassium pump	4.32×10^{-2} µM s^{-1}	[5]

Chloride flux through the chloride channel (in µM s^{-1}):

$$J_{Cl_i} = G_{Cli}\left(v_i - v_{Cli}\right) \tag{51}$$

G_{Cli}	Whole-cell conductance for Cl^- current	1.34×10^{-3} µM $mV^{-1}s^{-1}$	[5]
v_{Cli}	Reversal potential for Cl^- channels.	-25.0 mV	[5]

Potassium flux through potassium channel (in µM s^{-1}):

$$J_{K_i} = G_{Ki} w_i \left(v_i - v_{K_i}\right) \tag{52}$$

G_{Ki}	Whole-cell conductance for K^+ efflux.	4.46×10^{-3} µM $mV^{-1}s^{-1}$	[5]
v_{K_i}	Nernst potential	-94 mV	[5]

F_{KIR_i}	Scaling factor of potassium efflux through the KIR channel	750 mV μM^{-1}	[2]

Flux through KIR channels in the SMC (in µM s^{-1}):

$$J_{KIR_i} = \frac{F_{KIR_i} g_{KIR_i}}{\gamma_i}(v_i - v_{KIR_i}) \tag{53}$$

IP_3 degradation (in µM s^{-1}):

$$J_{degrad_i} = k_{di} I_i \tag{54}$$

k_{di}	Rate constant of IP_3 degradation	0.1 s^{-1}	[5]

Endothelial cell

Release of calcium from IP_3-sensitive stores in the EC (in µM s^{-1}):

$$J_{IP_{3j}} = F_j \frac{[IP_3]_j^2}{K_{rj}^2 + [IP_3]_j^2} \tag{55}$$

F_j	Maximal rate of activation-dependent calcium influx	0.23 µM s^{-1}	[5]
K_{rj}	Half-saturation constant for agonist-dependent calcium entry	1 µM	[5]

Uptake of calcium into the endoplasmic reticulum (in µM s^{-1}):

$$J_{ER_{uptake_j}} = B_j \frac{[Ca^{2+}]_j^2}{c_{bj}^2 + [Ca^{2+}]_j^2} \tag{56}$$

B_j	ER uptake rate constant	0.5 µM s^{-1}	[5]
c_{bj}	Half-point of the SR ATPase activation sigmoidal	1.0 µM	[5]

Calcium-induced calcium release (CICR; in µM s^{-1}):

$$J_{CICR_j} = C_j \frac{[\widehat{Ca}^{2+}]_j^2}{s_{cj}^2 + [\widehat{Ca}^{2+}]_j^2} \frac{[Ca^{2+}]_j^4}{c_{cj}^4 + [Ca^{2+}]_j^4} \tag{57}$$

C_j	CICR rate constant	5 µM s^{-1}	[5]
s_{cj}	Half-point of the CICR Ca^{2+} efflux sigmoidal	2.0 µM	[5]
c_{cj}	Half-point of the CICR activation sigmoidal	0.9 µM	[5]

Calcium extrusion by Ca^{2+}-ATPase pumps (in µM s^{-1}):

$$J_{extrusion_j} = D_j[Ca^{2+}]_j \tag{58}$$

D_j	Rate constant for Ca^{2+} extrusion by the ATPase pump	0.24 s^{-1}	[6]

Calcium flux through the stretch-activated channels in the EC (in µM s^{-1}):

$$J_{stretch_j} = \frac{G_{stretch}}{1 + e^{-\alpha_{stretch}(\sigma - \sigma_0)}}(v_j - E_{SAC}) = \frac{G_{stretch}}{1 + e^{-\alpha_{stretch}\left(\frac{\Delta pR}{h} - \sigma_0\right)}}(v_j - E_{SAC}) \tag{59}$$

$G_{stretch}$	The whole cell conductance for SACs	6.1×10^{-3} µM $mV^{-1}s^{-1}$	[5]
$\alpha_{stretch}$	Slope of stress dependence of the SAC activation sigmoidal	7.4×10^{-3} $mmHg^{-1}$	[5]
Δp	Pressure difference	30 mmHg	ME
σ_0	Half-point of the SAC activation sigmoidal	500 mmHg	[5]
E_{SAC}	The reversal potential for SACs	-18 mV	[5]

Leak current from the ER (in µM s^{-1}):

$$J_{ER_{leak_j}} = L_j[\widehat{Ca}^{2+}]_j \tag{60}$$

L_j	Rate constant for Ca^{2+} leak from the ER	0.025 s^{-1}	[5]

Calcium influx through nonselective cation channels (in µM s^{-1}):

$$J_{cation_j} = G_{cat_j}(E_{Ca_j} - v_j)\frac{1}{2}\left(1 + \tanh\left(\frac{\log_{10}[Ca^{2+}]_j - m_{3_{cat_j}}}{m_{4_{cat_j}}}\right)\right) \tag{61}$$

Potassium efflux through the $J_{BK_{Caj}}$ channel and the $J_{SK_{Caj}}$ channel (in µM s^{-1}):

$$J_{K_j} = G_{totj}(v_j - v_{Kj})\left(J_{BK_{Caj}} + J_{SK_{Caj}}\right) \tag{62}$$

G_{catj}	Whole-cell cation channel conductivity	6.6×10^{-4} µM $mV^{-1}s^{-1}$	[5]
E_{Caj}	Ca^{2+} equilibrium potential	50 mV	[5]
$m_{3_{catj}}$	Model constant	-0.18 µM	[5]
$m_{4_{catj}}$	Model constant	0.37 µM	[5]

G_{totj}	Total potassium channel conductivity.	6927 pS	[5]
v_{Kj}	K^+ equilibrium potential	-80.0 mV	[5]

Potassium efflux through the $J_{BK_{Caj}}$ channel (in µM s^{-1}):

$$J_{BK_{Caj}} = 0.2\left(1+\tanh\left(\frac{(\log_{10}[Ca^{2+}]_j - c)(v_j - b_j) - a_{1j}}{m_{3bj}(v_j + a_{2j}(\log_{10}[Ca^{2+}]_j - c) - b_j)^2 + m_{4bj}}\right)\right) \tag{63}$$

Potassium efflux through the $J_{SK_{Caj}}$ channel (in µM s^{-1}):

$$J_{SK_{Caj}} = 0.3\left(1+\tanh\left(\frac{\log_{10}[Ca^{2+}]_j - m_{3sj}}{m_{4sj}}\right)\right) \tag{64}$$

c	Model constant, further explanation see reference	-0.4 µM	[5]
b_j	Model constant, further explanation see reference	-80.8 mV	[5]
a_{1j}	Model constant, further explanation see reference	53.3 µM mV	[5]
a_{2j}	Model constant, further explanation see reference	53.3 mVµM^{-1}	[5]
m_{3bj}	Model constant, further explanation see reference	1.32×10^{-3} µM mV^{-1}	[5]
m_{4bj}	Model constant, further explanation see reference	0.30 µM mV	[5]
m_{3sj}	Model constant, further explanation see reference	-0.28 µM	[5]
m_{4sj}	Model constant, further explanation see reference	0.389 µM	[5]

Residual current regrouping chloride and sodium current flux (in µM s^{-1}):

$$J_{R_j} = G_{R_j}(v_j - v_{restj}) \tag{65}$$

G_{R_j}	Residual current conductivity	955 pS	[5]
v_{restj}	Membrane resting potential	-31.1 mV	[5]

IP_3 degradation (in µM s^{-1}):

$$J_{degrad_j} = k_{dj}[IP_3]_j \tag{66}$$

k_{dj}	Rate constant of IP_3 degradation	0.1 s^{-1}	[5]

Coupling

Heterocellular electrical coupling between SMCs and ECs (in mV s^{-1}):

$$V_{coupling_i}^{SMC-EC} = -G_{coup}(v_i - v_j) \tag{67}$$

Heterocellular IP_3 coupling between SMCs and ECs (in µM s^{-1}):

$$J_{IP_3-coupling_i}^{SMC-EC} = -P_{IP_3}([IP_3]_i - [IP_3]_j) \tag{68}$$

Calcium coupling with EC (in µM s^{-1}):

$$J_{Ca^{2+}-coupling_i}^{SMC-EC} = -P_{Ca^{2+}}([Ca^{2+}]_i - [Ca^{2+}]_j) \tag{69}$$

G_{coup}	Heterocellular electrical coupling coefficient	0.5 s^{-1}	ME
P_{IP_3}	Heterocellular IP_3 coupling coefficient	0.05 s^{-1}	[5]
$P_{Ca^{2+}}$	Heterocellular $P_{Ca^{2+}}$ coupling coefficient	0.05 s^{-1}	[5]

Additional Equations

Equilibrium distribution of open channel states for the voltage and calcium activated potassium channels (dimensionless):

$$K_{act_i} = \frac{([Ca^{2+}]_i + c_{wi})^2}{([Ca^{2+}]_i + c_{wi})^2 + \beta_i exp(-([v_i - v_{Ca_{3i}}]/R_{Ki}))} \tag{70}$$

Nernst potential of the KIR channel in the SMC (in mV):

$$v_{KIR_i} = z_1 K_p - z_2 \tag{71}$$

Conductance of KIR channel (in µM mV^{-1} s^{-1}):

$$g_{KIR_i} = exp(z_5 v_i + z_3 K_p - z_4) \tag{72}$$

5.3 The Contraction Model

Fraction of free phosphorylated cross-bridges (dimensionless):

$$\frac{\mathrm{d}[Mp]}{\mathrm{d}t} = K_4[AMp] + K_1[M] - (K_2 + K_3)[Mp] \tag{73}$$

c_{wi}	Translation factor for Ca^{2+} dependence of K_{Ca} channel activation sigmoidal.	0.0 µM	[5]
β_i	Translation factor for membrane potential dependence of K_{Ca} channel activation sigmoidal.	0.13 μM^2	[5]
$v_{Ca_{3i}}$	Half-point for the K_{Ca} channel activation sigmoidal.	-27 mV	[5]
R_{Ki}	Maximum slope of the K_{Ca} activation sigmoidal.	12 mV	[5]
z_1	Model estimation for membrane voltage KIR channel	4.5×10^3 $mV\mu M^{-1}$	[1]
z_2	Model estimation for membrane voltage KIR channel	112 mV	[1]
z_3	Model estimation for the KIR channel conductance	4.2×10^2 $mV^{-1}s^{-1}$	[1]
z_4	Model estimation for the KIR channel conductance	12.6 µM $mV^{-1}s^{-1}$	[1]
z_5	Model estimation for the KIR channel conductance	-7.4×10^{-2} µM $mV^{-2}s^{-1}$	[1]

Fraction of attached phosphorylated cross-bridges (dimensionless):

$$\frac{\mathrm{d}[AMp]}{\mathrm{d}t} = K_3[Mp] + K_6[AM] - (K_4 + K_5)[AMp] \tag{74}$$

Fraction of attached dephosphorylated cross-bridges (dimensionless):

$$\frac{\mathrm{d}[AM]}{\mathrm{d}t} = K_5[AMp] - (K_7 + K_6)[AM] \tag{75}$$

Fraction of free non-phosphorylated cross-bridges (dimensionless):

$$[M] = 1 - [AM] - [AMp] - [Mp] \tag{76}$$

Rate constants that represent phosphorylation of M to Mp and of AM to AMp by the active myosin light chain kinase (MLCK), respectively (in s^{-1}):

$$K_1 = K_6 = \gamma_{cross}[Ca^{2+}]_i^{n_{cross}} \tag{77}$$

K_2	Rate constant for dephosphorylation (of Mp to M) by myosin light-chain phosphatase (MLCP)	0.5 s^{-1}	[4]
K_3	Rate constants representing the attachment/detachment of fast cycling phosphorylated crossbridges	0.4 s^{-1}	[4]
K_4	Rate constants representing the attachment/detachment of fast cycling phosphorylated crossbridges	0.1 s^{-1}	[4]
K_5	Rate constant for dephosphorylation (of AMp to AM) by myosin light-chain phosphatase (MLCP)	0.5 s^{-1}	[4]
K_7	Rate constant for latch-bridge detachment	0.1 s^{-1}	[4]
γ_{cross}	Sensitivity of the contractile apparatus to calcium	17 μM^{-3} s^{-1}	[6]
n_{cross}	Fraction constant of the phosphorylation crossbridge	3 [–]	[6]

5.4 The Mechanical Model

Wall thickness of the vessel (in µm):

$$h = 0.1R \tag{78}$$

Fraction of attached myosin cross-bridges (dimensionless):

$$F_r = [AM_p] + [AM] \tag{79}$$

Vessel radius (in m):

$$\frac{\mathrm{d}R}{\mathrm{d}t} = \frac{R_{0_{pas}}}{\eta}\left(\frac{RP_T}{h} - E(F_r)\frac{R - R_0(F_r)}{R_0(F_r)}\right) \tag{80}$$

with:

$$E(F_r) = E_{pas} + F_r\left(E_{act} - E_{pas}\right) \tag{81}$$

$$R_0(F_r) = R_{0_{pas}} + F_r(\alpha - 1)R_{0_{pas}} \tag{82}$$

η	viscosity	10^4 Pa s	[5]
$R_{0_{pas}}$	Radius of the vessel when passive and no stress is applied	20 µm	ME
P_T	Transmural pressure	4×10^3 Pa	ME
E_{pas}	Young's moduli for the passive vessel	66×10^3 Pa	[3]
E_{act}	Additional component of the Young's moduli when vessel is active	167×10^3 Pa	[3]
α	Scaling factor initial radius	0.6	[3]

References

[1] **Filosa, J. a.; Bonev, A. D.; Straub, S. V.; Meredith, A. L.; Wilkerson, M. K.; Aldrich, R. W. and Nelson, M. T.** (**2006**): Local potassium signaling couples neuronal activity to vasodilation in the brain., Nature neuroscience, Vol. 9, No. 11 pp. 1397–1403.

[2] **Gonzalez-fernandez, J. M. and Ermentrout, B.** (**1994**): On the origin and dynamics of the vasomotion of small arteries, Mathematical biosciences, Vol. 119, No. 2 pp. 127–167.

[3] **Gore, R. W. and Davis, M. J.** (**1985**): Mechanics of Smooth Muscle in Isolated Single Microvessels, Vol. 12 pp. 511–520.

[4] **Hai, C.-m. and Murphy, R. A.** (**1989**): Ca2+ Crossbridge Phosphorylation, and Contraction, Annual review of physiology, Vol. 51, No. 1 pp. 285–298.

[5] **Koenigsberger, M.; Sauser, R.; Bény, J.-L. J. and Meister, J. J.-J.** (**2006**): Effects of arterial wall stress on vasomotion, Biophysical journal, Vol. 91, No. September pp. 1663–1674.

[6] **Koenigsberger, M.; Sauser, R.; Bény, J.-L. L.; Meister, J.-J. J. and Be, J.-l.** (**2005**): Role of the endothelium on arterial vasomotion, Biophysical journal, Vol. 88, No. 6 pp. 3845–3854.

[7] **Nagelhus, E.; Horio, Y. and Inanobe, A.** (**1999**): Immunogold evidence suggests that coupling of K+ siphoning and water transport in rat retinal muller cells is mediated by a coenrichment of kir4. 1 and aqp4 in specific membrane domains, Glia, Vol. 63, No. 1 pp. 47–54.

[8] **Ø stby, I.; Ø yehaug, L.; Einevoll, G. T.; Nagelhus, E. A.; Plahte, E.; Zeuthen, T.; Lloyd, C. M.; Ottersen, O. P. and Omholt, S. W.** (**2009**): Astrocytic Mechanisms Explaining Neural-Activity-Induced Shrinkage of Extraneuronal Space, PLoS Computational Biology, Vol. 5, No. 1 pp. 1–12.

[9] **Shipp, S.** (**2007**): Structure and function of the cerebral cortex., Current biology : CB, Vol. 17, No. 12 pp. R443—-9.